Reduced-Gravity Simulator for Field Environments -Drone Augmented System

May 2022

Final Report

Faculty Advisor: Jason Lee (ME), Patrick Kumavor (BME)

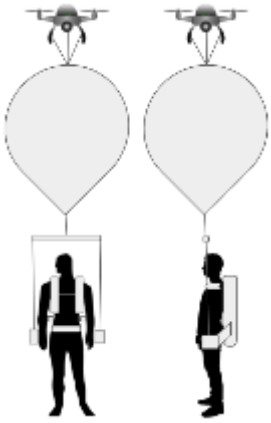

Team ME 30:

Peter Stokes, Allison Tewksbury, Joseph Lee

BME Teammates:

Changhun Lee, Norlinda Steward, Randall Radcliff

i. Abstract

Astronauts need to go through extensive training on Earth before heading into space, and the more accurate the analogue, the better prepared they will be. NASA currently trains astronauts in simulated lower gravity environments in either the Neutral Buoyancy Laboratory or the Active Response Gravity Offload System (ARGOS), but neither of these systems allow for testing outdoors in field environments. NASA, in partnership with Aquiline Drones, mechanical engineering, biomedical engineering, and the Krenicki Arts and Engineering Institute, are working to develop a gravity offload device compatible with testing in field environments such as Desert Research and Technology Studies (Desert RATS). This report covers the technical requirements of the gravity offload device, the design choices and justifications, options for scalability, current progress, and future goals. Two separate teams were formed to respond to NASA's solicitation, and this report covers the work of the weather balloon and drone side of the project. Using a weather balloon to passively offload the user's weight and a drone to actively respond to changes using a series of sensors, this system should create a consistent and well balanced offloading force. The weather balloon and drone system is connected to a harness system to comfortably lift the user, offload at their center of gravity, and provide attachment points for some of the necessary sensors. Final testing proved the comfort of the harness, mobility of the user, and passive stability of the balloon offload to exceed all expectations of the team. The current system is a scaled model of what NASA would be able to implement with a maximum offload of 25 pounds. The ability to scale up to NASA's desired value of 100 pounds is easily achievable with linear scaling of the current model. All systems should work similarly on scaled versions, but minor tweaking and enhanced controls would be needed for optimal performance.

ii. Table of Contents

i. Abstract i

ii. Table of Contents ii

iii. Table of Figures iv

iv. Table of Tables v

v. Nomenclature Glossary vi

1 Introduction 1

2 Problem Statement 2

2.1 Statement of Need 2

2.2 Requirements 2

2.3 Basic Limitations/Specifications 3

2.4 Verification Approach 4

3 Theory 6

3.1 Governing Equations 6

4 Results/Design/Analysis 8

4.1 Design Process 8

4.2 System Definition 12

4.3 Testing 20

4.4 Results 25

5 Summary 32

6 References 33

6.1 Works Cited 33

6.2 Works Consulted 33

7 Appendix A- Matlab Code 35

7.1 Appendix A1- Matlab Code for Drone time of flight 35

7.2 Appendix A2- Matlab Code for Drag force on balloon 35

7.3 Appendix A3- Matlab Code for percent error in the unit problem 36

8 Appendix B- Unit Problem 37

iii. Table of Figures

Figure 1. Time of Flight vs Weight of Drone 10

Figure 2. Balloon size vs Lifting Force 11

Figure 3. Drag Force vs Wind Speed 12

Figure 4. CAD Model of Full System 13

Figure 5. Drone Tether Fabrication 15

Figure 6. Fabricated Gimbal Annotated 16

Figure 7. Sensor Diagram 17

Figure 8. Stress/Strain of Gimbal 18

Figure 9. Hercules 2 Drone 18

Figure 10. Hercules 10 Drone 19

Figure 11. Drone Stability Testing Outdoors 21

Figure 12. Drone Stability Flight Data 21

Figure 13. Small Scale Netting 23

Figure 14. Drone and Net Tension Testing 24

Figure 15. Full Scale Testing Photos 25

Figure 16. Sensor System Diagram 27

Figure 17. One Balloon 30

Figure 18. Multiple Balloons 31

Table of Tables

Table 1. Pugh Chart for Offloading Technologies 5,9

iv. Nomenclature Glossary

ARGOS - *Active Response Gravity Offload System. This is an indoor facility in NASA Johnson in Houston, TX with the ability to offload the weight of a user in order to perform tests in different simulated gravity environments.*

Desert RATS- *Desert Research and Technology Studies*

EMU - *Extravehicular Mobility Unit. This is the type of spacesuit worn by astronauts while performing an EVA.*

EVA - *Stands for "Extravehicular Activity". This is the name for any activity that an astronaut performs outside of their vehicle while in space.*

FEA - *Finite Element Analysis. Analyzing a system using software that breaks the calculations down into smaller pieces that can be numerically and independently calculated before being brought together to get the full picture.*

Gimbal - *A rigid frame used to fix the upward force from a gravity offload device around the center of gravity of a user.*

1 Introduction

The purpose of this report is to document the process of determining the best method of offloading weight in a field environment for the purpose of simulating Lunar (⅙ Earth's) or Martian (⅓ Earth's) gravity. The field environment is described as a desert-like climate such as a Desert RATS site in Northern Arizona. The system must be able to navigate the intense terrain of this environment. NASA does not currently have the capability of simulating reduced gravity in these desert-like field environments for training purposes. The capability of simulating the environment will need to be achieved in order for astronauts to be adequately prepared for future missions to the Moon and Mars. Currently, NASA has programs such as ARGOS as well as the Neutral Buoyancy Laboratory, but these are stationary. There are two separate teams working on developing a more mobile system; one is developing a mobile frame system and we are making a drone-augmented system. We need to offload forces scalable to at least 100 lbf by exploring the options of weather balloons, drones, or some other system. We determined the most effective method of simulating ⅙ of gravity and provided a concept that can be used in testing. In order to frame our work, requirements were created with reference to the problem statement as well as assumptions made about the system. Our drone-augmented weather balloon system can offload 25 lbf in a field environment, is safe for an astronaut, allows all relevant movements for training, and actively responds to movement and changes in the center of gravity. The weather balloon provides a passively stable weight offload, a custom made harness/gimbal system offloads weight comfortably at the user's center of mass, and a sensor provides controller inputs to a drone to actively move the system to respond to the user. Final testing achieved all of these goals with the exception of implementation of the sensor inputs. The sensors were incorporated into the system ready to be used, but final code to control the drone was not finalized by project end. The final results showed how our system is centered around

simplicity, uses basic systems with high reliability, and is completely unaffected by ground conditions. This makes for a highly promising field environment gravity offload device.

2 Problem Statement

2.1 Statement of Need

The current technology used for simulating reduced gravity are not capable of being used in field environments. The current technology consists of ARGOS and the Neutral Buoyancy Laboratory, which both can simulate Martian or Lunar gravity, but cannot be used outdoors or in rough terrain. We aim to develop a method of simulating reduced gravity that is scalable to 100 lbs that can be used outdoors in a desert-like climate. It is necessary to test in this climate because future space exploration will be carried out with the Moon to Mars program beginning in 2024. Simulating Martian or Lunar terrain will be necessary in order to prepare astronauts for this mission and more.

2.2 Requirements

2.2.1 Our concept shall be able to offload 25 pounds of force.

2.2.2 It shall be able to be used in a desert-like field environment such as the Desert RATS sites in northern Arizona.

2.2.3 The design shall be safe and wearable for an astronaut in training.

2.2.4 The design shall enable relevant movement, such as standing, sitting, bending over, jumping, and walking.

2.2.5 The design shall actively respond to movement and change in the center of mass in order to provide a consistent offloading force. The controls are customizable to our needs.

2.2.6 The harness shall be comfortable to the wearer by not having any major points of pressure. It should offload the appropriate percentage of the user's weight. The harness shall also be compatible with an extravehicular mobility unit (spacesuit worn on EVAs).

2.2.7 The weather balloon shall use helium as a lifting gas and be able to be calibrated within a pound of accuracy of lifting force.

2.3 Basic Limitations/Specifications

2.3.1 There must be a tethered connection from the drone to the controller and harness due to latency issues. Ideally, we would want a wireless connection between the drone and harness sensors, but because the response time necessary is minimal, a wireless connection would not have the same level of functionality and control.

2.3.2 FAA regulations dictate which settings we can perform tests in as well as necessary testing procedures.

2.3.2.1 All parts of the system must be attached at takeoff, because any attempt to work on the system with an active drone is a massive safety hazard. The takeoff condition of the system is going to be entirely horizontal on the ground with plenty of room for the weather balloon to stay a safe distance from the fan blades.

2.3.2.2 Outdoor testing must be performed with a licensed P107 pilot. While the pilot will be provided upon request, it is also a limitation that we cannot perform spontaneous testing. Proper planning will be critica due to the need to contact a pilot beforehand.

2.3.2.3 The drone cannot be flown directly above a human during any point. Aquiline Drones's commercial drones are not certified to fly over people, so we will be using a mannequin for all testing. Two different mannequins (inflatable and solid) will be used during different phases. The drone used in full scale testing would need to meet the proper certifications before being used to fly over a person.

2.3.3 Scalability of our design is critical. We will provide proof of concept which can be expanded on in order to offload the entire sum of 100 lbs as written in NASA's original proposal.

2.4 Verification Approach

Beginning the project, the mechanical team brainstormed numerous methods of offloading a person's weight. NASA requested novel and creative concepts, so we had to propose and subsequently pare down the ideas. We utilized a Pugh chart as seen below in table 1 to compare how each idea performed on all relevant metrics with relative weightings on each category to accurately represent their importance.

Table 1: Pugh chart comparing different offloading technologies

Criteria	Weight	Drones	Balloons	Cold Gas Thruster	Pulley	Aerated Fluid	Drones and Balloons
Feasibility	1	3	3	1	3	2	3
Able to lift 25 lbf	1	2	2	3	3	2	3
Useful in Field Environment	2	3	3	3	1	1	3
Safety	2	2	3	1	3	2	3
Enable movement	2	3	2	1	1	1	3
Controls	1	2	3	1	3	3	2
Actively responds to changes	1	3	2	1	1	3	3
Scalability	2	1	2	1	3	3	3
	Sum	**28**	**30**	**18**	**26**	**24**	**35**

Once a design was selected, we needed to verify our three main requirements of weight offload, active control, and harness attachment. Weight offloading through the weather balloon can be verified with buoyancy calculations, as it is a simple system. If the final weight offload value measured through a spring scale differs from the desired value, the volume of helium can be adjusted on the fly. The active controls using the drone would be verified through manual perturbations of the system and tweaking the response of the drone until it is stabilized within our allowed latency and margin of error. A closed loop feedback system between the sensors and the drone would continuously update the drone's position and keep the system stable. Finally, the harness was tested on a person to ensure it is comfortable and

supporting, and then tested on the mannequin during tests to ensure it translates the offloading in the desired direction.

3 Theory

One of the expectations of our gravity offload device was for it to be a novel concept. This means we could not base our idea entirely on the existing gravity offload devices, but we needed to know about the limitations and innovations of the existing technologies. To help accomplish this, we spoke to employees who work at both the NASA ARGOS and the Neutral Buoyancy Lab. The ARGOS team told us that the longer the tether for our offload device, the more control authority it will have over the system. This means we can increase lever length if we need to have increased control over the system. The ARGOS team also shared how their harnesses/gimbals typically include rigid structures around the user that allow the attachment points to be near the center of gravity for the user. This helps maintain the balance and consistency of the weight offload. The largest limitations of the ARGOS and Neutral Buoyancy Lab's facilities were both described to be the lack of mobility and usability in field environments. The most important problem we need to address is ensuring mobility and usability across field environments such as Desert RATS.

3.1 Governing Equations

One of the biggest testing constraints within our system is the amount of time the drone can be in flight before running out of battery. The time of flight given by a standard drone is shown in Equation 1

$$T = CDV/(mP) \quad [1]$$

$$F_d = 0.5 C_d A \rho v^2 \quad [2]$$

where F_d is the drag force (lbs), C_d is the coefficient of drag, A is the cross-sectional area of the balloon (ft^2), ρ is the density of air (lbm/ft^3), and v is the velocity of wind (ft/s).

Sizing the weather balloon is dependent on the buoyant force achieved at any given balloon radius. The buoyant force of a lifting gas is given by Equation 3 below

$$F_B = (\rho_{air} - \rho_{gas}\ ) * gV \quad [3]$$

where F_B is the Buoyant Force (lbf), ρ_{air} is the density of air, $\rho_{gas}$is the density of lifting gas, g is the acceleration of gravity (ft/s^2), and V is volume (ft^3). Results from these equations can be found in Section 4.

4 Results/Design/Analysis

4.1 Design Process

The first step in creating a solution to the problem was to brainstorm a variety of ideas that could successfully meet the goals of the project. We then leveraged a Pugh chart as a method of determining which would be the best solution given requirements. We came up with many requirements the system must be able to accommodate, and weighted every requirement that NASA specifically requires to be twice as important as our other requirements. We ranked each system on a scale from 1-3 (unweighted) for each of our requirements, and summed up the scores from each system. The option with the highest score represents the most viable system. Based on our grading, drones used in conjunction with balloons was the best choice, with its only perceived weakness to be the implementation of controls. This pugh chart can be seen below in table 1. Criteria was weighted based on what was explicitly stated in the project statement, with higher values for use in field environments, safety, enabling movement, and scalability. The rest of the criteria were important but not necessary to meet the goals of the project.

Table 1: Pugh chart comparing different offloading technologies

Criteria	Weight	Drones	Balloons	Cold Gas Thruster	Pulley	Aerated Fluid	Drones and Balloons
Feasibility	1	3	3	1	3	2	3
Able to lift 25 lbf	1	2	2	3	3	2	3
Useful in Field Environment	2	3	3	3	1	1	3
Safety	2	2	3	1	3	2	3
Enable movement	2	3	2	1	1	1	3
Controls	1	2	3	1	3	3	2
Actively responds to changes	1	3	2	1	1	3	3
Scalability	2	1	2	1	3	3	3
	Sum	**28**	**30**	**18**	**26**	**24**	**35**

The two other top options were drones and balloons, separately. Drones by themselves were mostly limited by their lack of scalability, one of the most important metrics we looked at. Not only are there significant limitations to the payload capacity of drones, meaning this type of system would likely need a swarm of heavy lift drones, but as one increased the weight offloaded by each drone, the drone's flight time would drop significantly. The more weight a drone carries, the more power it consumes, and the quicker it depletes its battery. Figure 1 shows a rough estimate of the time of flight vs the weight lifted by a generic drone. This graph utilizes equation 1 to show the general trend in increasing the payload of a drone. NASA's training for EVAs are typically on the order of multiple hours, and most of the drones we looked at have a flight time of less than an hour with no payload. This would fall dramatically

once weight was added, so even if a swarm of enough drones was assembled to lift the required weight, the flight time would be less than what an actual astronaut would need to train with.

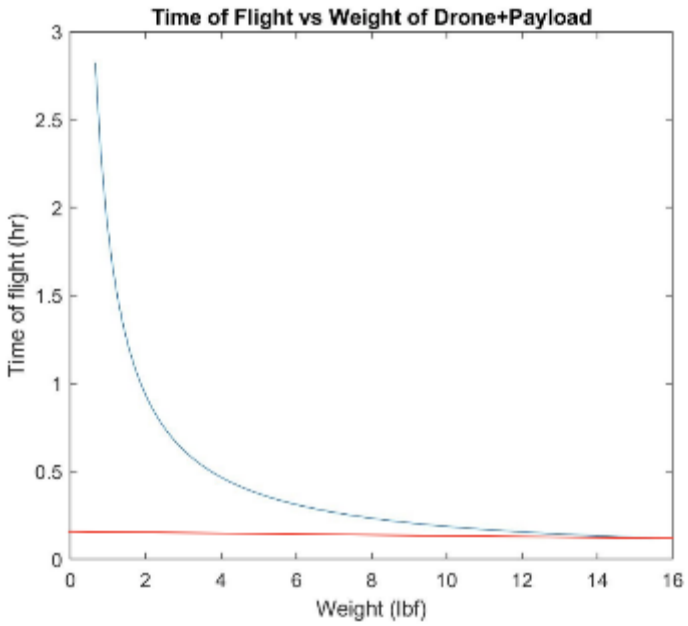

Figure 1: Time of flight vs weight of a drone plus its payload using equation 1. The red line in the plot shows that lifting 15 pounds of weight with a drone will reduce the flight time to about 10 minutes.

The second highest ranked option from our Pugh chart was a balloon by itself. The biggest weakness of this option was lacking active controls. Balloons have been used to lift weight for decades. In 1973, the military explored using a large balloon attached to a tether where the weight would be pulled laterally with the balloon [1]. The load capacity for this balloon was over ten tons. This system has been used in the logging industry which makes it possible to carry large fallen trees over uneven terrain. The military conducted testing for this concept, although it was ultimately discarded in favor of a crane system. They noted that there were several logistical issues at the time with transporting all of their equipment as well as the cost of helium, which has only gotten more expensive in the past 50 years. Since we do not need to offload 10 tons, the cost of helium is not a major concern. Although balloons are not used in lifting cargo today, such a large balloon lift capacity is notable, and the tethered lateral

approach was not something we had considered for our balloon system. This being said, we had concerns about the ability for a balloon to offload enough weight for the system to be scalable. In order to verify scalability, we performed buoyancy calculations for a balloon in air. Figure 2 shows equation 3 graphed as lifting force vs radius of a balloon. It also explores the difference between hydrogen and helium as buoyant gasses. A green line was added to show our desired lifting force of 25 lbf. The intersection of the green line and the helium curve tells us that a balloon would need to be around 9ft in diameter to offload the weight we will see in our tests, which is allowable within the constraints of a typical weather balloon. This system is also scalable to 100lbs or more for NASA.

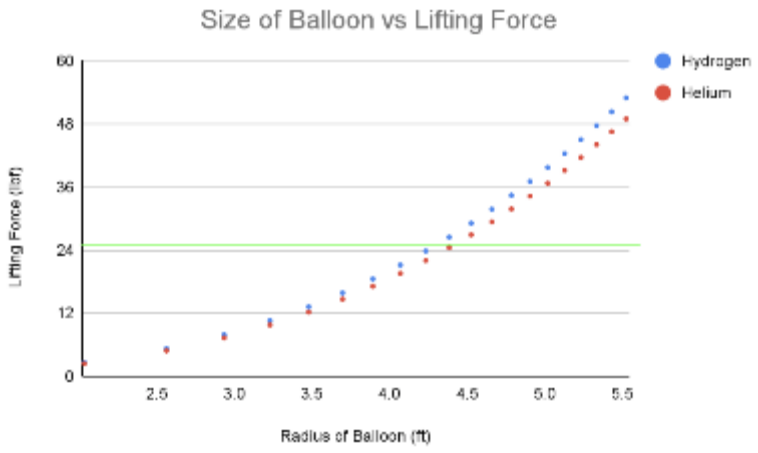

Figure 2: Plot of balloon size vs lifting force calculated using Equation 3.

The biggest advantage of a drone and weather balloon system over just a balloon system is the ability for active control. In order to control the balloon with a drone, we needed to verify the power of the drone is enough to move the balloon as desired. One of the main forces the drone must contend with is the drag force of the balloon as the user walks around. The drone should be able to pull the balloon forward so it remains directly over the center of gravity of the user even as the user walks around. Using equation 2, we were able to calculate the approximate drag forces this balloon will experience due to air

resistance. The results are graphed in figure 3. The average walking speed is about 3-4 miles per hour, so if a drone can lift over 1.5lbf, then we can be confident that it can control the balloon well.

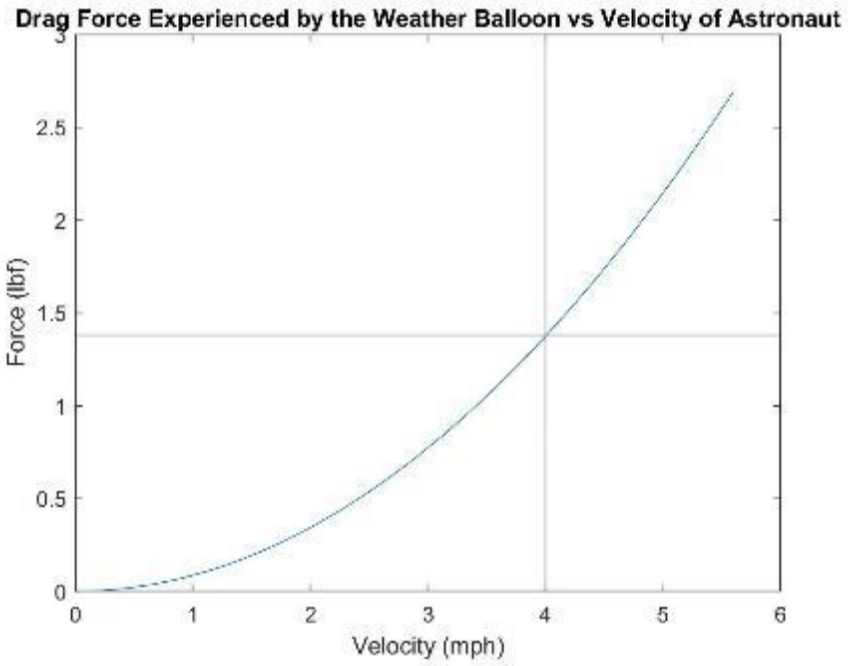

Figure 3: Plot of drag force vs wind speed calculated using Equation 2 and executed using MATLAB code listed in Appendix A1.

4.2 System Definition

In creating a system, it was important to visualize the relative sizing of all the components, as well as assemble them together to see how they connect. In figure 4 we modeled our design with all three subsystems to scale. The top of the image shows the drone, the middle is the weather balloon, and the bottom shows the harness. This is a general layout that can be used for qualitative analysis of designs.

Figure 4: A Computer Aided Drawing of the system design to scale. The drawing consists of the drone (1), weather balloon (2), and harness (3)

Label 3 in Figure 4 is the harness. This harness is being developed by the BME team, which focuses on weight distribution and targeting the Center of Mass of the astronaut. The harness consists of three components - a full body climbing harness, an external frame backpack, and a beam. The climbing harness distributes the load on the individual safely, from the thighs to the chest. It will be able to support the astronaut comfortably and while jumping in the air as it was designed to suspend an individual using a tether. An external frame backpack is utilized to accept the load from above and

position the connection points according to the center of gravity. With the backpack being lightweight, it is a useful platform for fabricating varying connection points. As a backpacking backpack, it also has shoulder, chest, and hip straps for comfort on the astronaut. The beam is suspended above the individual, and is used to position the tether from the weight offload system to the harness. For more information on the harness please refer to BME Team 10's Project Report 3 for their full analysis.

In the middle of the figure is the weather balloon. It provides the lift of the system and is sized at 9 feet in diameter for 25 pounds of lift. The lifting gas calculations seen in the results section explains the reasoning behind this balloon size. The constraints that define these values can be found in section 4. The tether material used we selected is 550 paracord. It is tethered to the harness subsystem by the beam. It is modeled 8 feet above the harness' swivel bar and 6 feet below the drone to allow room for relative motion between each of the components. The tethers attach to the weather balloon by carabiners as well as potentially netting. During a test, the weather balloon lifts the subject, and naturally does not move very far from the astronaut when they are in motion, and at most is slightly pulled from below in the direction of movement. To accommodate for this, the drone above is activated to apply a force on the top of the balloon while following the movement of the person. Overall, there are two system forces applied to the balloon, which aim for a neutral and stable position of the balloon above the center of gravity of the astronaut.

The active control within our system will come from the drone and its connected sensors. The selected drone is the Hercules 2- chosen because it exceeds all necessary performance metrics and our sponsor Aquiline Drones has one available for use. The Hercules 2 can be programmed to take input from external sensors, has low latency, and can lift a payload of over a pound. Because the strongest parts of the drone are the arms, one tether is attached to each arm to create a symmetric load on the drone. The tether design was tested for different materials, connection methods such as carabiners and knots, and location of attachment points. These tethers help the drone control the weather balloon based on input

from the sensors within the harness. The final selection was based on tether systems used by helicopters to carry payloads underneath the vehicle. The layout and design can be seen in figure X below.

Various knots, hitches, and braids are used to fabricate the tethers. Each was chosen specific to its purpose. The bowline knot is used to attach a rope to a bar and provides good strength. The square knot is used to connect two same-diameter ropes together, and is used for four ropes in series. The four stranded braid is used to join four same-diameter ropes together to make one large rope and provides a concise attachment point under the drone's center of gravity. The four strand eye splice takes the four stranded braid and converts it into a loop to have one line of rope descend down from the drone. The rolling hitch is used to connect a rope to a closed loop. The cat's paw hitch strongly connects a line of rope to a carabiner. The carabiner is the attachment point to the top of the netting.

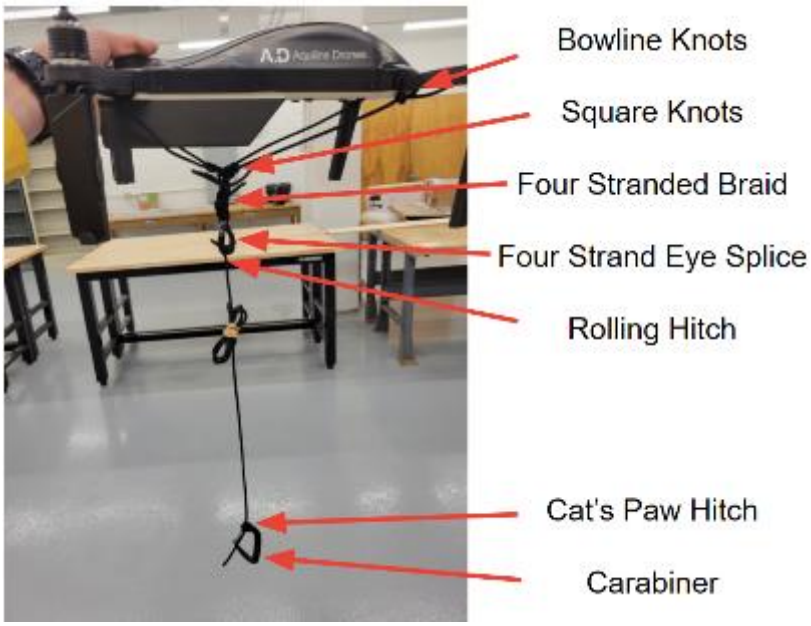

Figure 5: Tether design used to connect the drone to the netting on the balloon. Each location in the tether has a different type of knot labeled on the right.

The netting is used to connect the weather balloon to the drone and the harness. The netting is thin-roped nylon that has 550 paracord around the perimeter of the netting, with each corner fastened with carabiners for attachment points.

Initially, Sensors were located on each side of the harness in the arms as well as one in the backplate as seen in figures 5A and 5B. The data from these sensors would have been combined with data from the drone's internal sensors to dictate its motion. By moving the weather balloon, the drone would be able to change the balance of the system in order to keep it stable and working as intended. Upon testing, it was found that the sensor type purchased was not able to keep up with translational movement with its GPS as quickly as needed with this system. The BME pivoted their system to take advantage of the gyroscope's capabilities instead.

Figure 6: Gimbal system fitted to the mannequin.

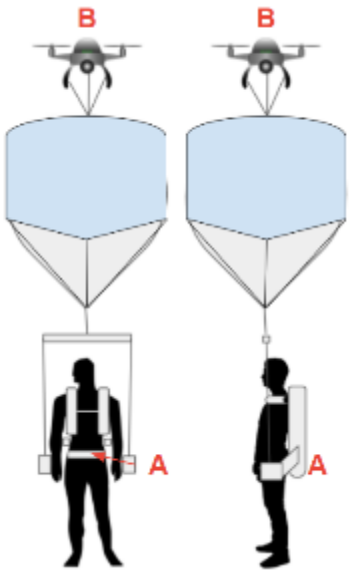

Figure 7: Diagram of full system setup with sensors A & B labeled.

Some of the largest loads of the system will exist within the gimbal and harness attachments. The BME team designed the gimbal to accommodate the expected loads plus a factor of safety. In order to predict how the gimbal design will react under expected conditions, the BME team conducted a SOLIDWORKS simulation. The simulation was done under the following assumptions: the part is constructed from a mild steel alloy, the part has a force of 100 lbf applied to each of the arms, and finally that the back of the gimbal is fixed. The simulation resulted in the following stress and strain diagrams seen in figure 8 below. Note: the exact design of the harness was understood to change, but this analysis shows both the high stress points for comfort and structural rigidity perspectives. Our loads would be well within the margins of materials chosen.

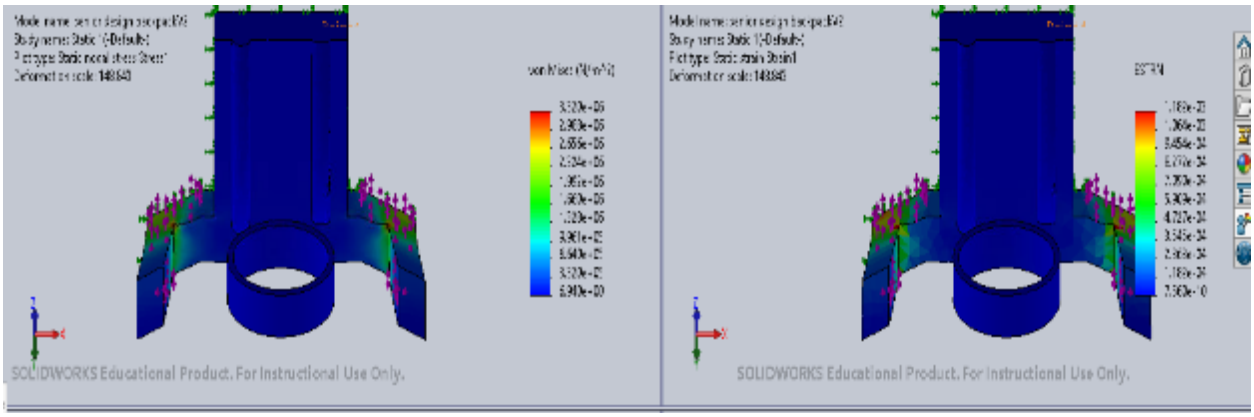

Figure 8: Stress and strain simulations of the gimbal model

The critical points of the design are found in elbows of the anchoring arms. Further optimizations to the design would likely be reducing the angle of the elbows to a gradual curve and cutting sections of the back plate for weight reduction. Reducing the angle of the elbows would help reduce the stress and strain hot spots, and weight reduction helps the system perform better and more efficiently.

Our sponsor, Aquiline Drones, offered the use of two different drones for our project. The options were Hercules 2 shown in figure 7 and Hercules 10 as shown below in figure 8.

Figure 9: Hercules 2 drone.

Figure 10: Hercules 10 drone.

We chose the Hercules 2 Drone because the control capacity compared to the Hercules 10 was closer to the desired specifications listed in our work breakdown structure. Even though the Hercules 2 is able to only lift 1 pound, this is to apply force to the weather balloon to guide it into the correct position. The rotors utilized in the drone provide more than sufficient lift. Due to the mass of the camera and gimbal, they can be removed from the drone to increase the payload capacity and improve performance to the numbers mentioned in section 4. However, when the camera and gimbal are removed, its center of mass changes and it requires sufficient modifications to its code in order for the drone to be able to stabilize itself. If we allow for slower accelerations, the Hercules 2 is more than capable of moving the balloon in the required ways. The Hercules 2 also has generally fantastic stabilization. The Hercules 10 drone is more capable of lifting, but its high cost of $20,000 makes it too high a risk for minimal performance trade-off. It is far lower risk and far more convenient to use the Hercules 2. On full scale systems for NASA, larger drones like the Hercules 10 may become worth the additional cost and risk.

One of the most important components of this project was to determine the various attachment points and methods to connect all the components together. There are three main subsystems that need to be connected within our system and each has a variety of attachment options. Between the harness and the balloon there are a couple problems to solve. The gimbal arms have attachment points on either side of the user's hip, so tethers anchoring to the arms need to be consolidated to symmetrically attach to the balloon subsystem. Due to overinflating the balloon to increase sea level lift, we cannot use a single attachment on the neck of the balloon as would normally be done. To solve this problem, we created multiple net systems to distribute the force over the surface of the entire balloon to test for efficacy. Each of these net systems were also evaluated for their ability to provide attachment options to the drone's tether above. Each of the subsystems require connection solutions that must optimize the interface in both directions. For the drone tethers, we have settled for close-belly tethers from the drone arms which transitions to a helicopter remote hook tether rig to connect to the weather balloon. Tether material is 550 paracord, where various knots are connection points between paracord.

4.3 Testing

The inflatable mannequin test is a lightweight, full volumetric setup that allows us to see how the system responds. We focus on the tethers of the drone to the weather balloon and the harness, to test new configurations to see which works best. We focused on metrics of responsiveness, accuracy, and stability. Responsiveness is the time it takes for drone movement to translate into weather balloon movement, as different tethers will yield varying times. Accuracy is the matching of translation in the x and y plane of the drone movement to the weather balloon movement and the difference between desired weight offload and actual offload values. Stability is the ability of the system to regain equilibrium after experiencing perturbations, ability to maintain the desired offload through movement of the

mannequin, and the ability to continue consistent offloading throughout the duration of the test. In addition, we used the results to refine logistics such as the takeoff and landing procedures. The drone proved to be remarkably stable with no controller input. It was able to fly at a hover in high wind conditions (see Figure 11).We can also examine the flight data to see the drone's response and active stability.

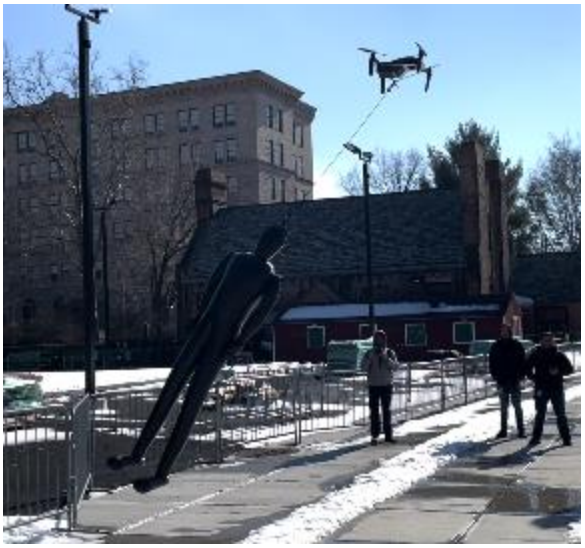

Figure 11: The drone takes off while attached to the inflatable mannequin laying horizontally and hovers above it. The mannequin is seen being held at an angle by the wind while the drone keeps it stationary.

Figure 12: The drone (green) is stable during no controller input until the drone pilot (red) begins to land.

To control the system, we first utilized manual control of the drone through a pilot. The pilot centers the drone above the harness through continuous movement so that the weather balloon will be centered above the harness. Through understanding system operations, we can seek to automate the interaction between the position of the harness and the drone. Any problems discovered in manual pilot flight will be addressed then, and considered in the automated process. This is accomplished using a triangularization algorithm, and is referenced from the BME team report. In order to have an active control system, the position and movement of the astronaut needs to be measured and tracked. The most important metrics of a tracking system for this application are accuracy, latency, and ability to track through somewhat complex movements. In a 2006 study, markers were placed on the joints of rock climbers and tracked with 6 infrared cameras [2]. During the trials, climbers would move rapidly with articulations at every joint. The infrared tracking system effectively created a 3-D model of their body during these movements in an outdoor environment and calculated the center of mass. Nine segments were created from the markers and tracked for easier data manipulation. Trunk and head, arms, forearms, thighs, and legs were all tracked as separate entities. The center of mass of each segment could be calculated from the x, y, and z coordinates of each marker, and the center of mass of the person could be computed from the average of each segment. This level of detail, knowing the movement of every joint, would not be necessary for the controls of a gravity offload device. A system of reduced complexity could still provide a useful center of mass data for the drone. Testing for this system would entail moving the center of mass by a certain length (a few inches, a few feet, and a longer distance) and timing how long it takes for the system to adjust itself to move directly over the center of mass. The test consists of multiple trials where the time of response may vary with the distance moved. A response time above our defined values would indicate an issue within our system. We will follow debugging steps to locate bottlenecks between sensing and reaction, and implement improvements as we find them. Continuous improvements will be made to streamline the system until the system's latency is acceptable.

There was also a great deal of consideration in regards to selecting a netting material that would distribute the force onto the balloon. At over 100 square feet of contact between a potential netting and fragile latex balloon, it was important that friction was not too much or that any single points were providing too much of a pressure point. The first material we considered was a polyethylene sheeting because of its smoothness and supposed strength (the same material is used in a garbage bag and it is meant to withstand a fair amount of weight without ripping). We purchased multiple materials, including this polyethylene sheeting, sports netting, bird nets (used in gardens), and more. A tensile strength test was performed on each using a strain gauge and pulling on the material. There was also a qualitative friction test where a similar latex balloon was rubbed against the material. The polyethylene did poorly on the tensile strength test, so we settled on a black netting that did well in both categories. A smaller version of about 3 ft by 3 ft was fabricated where we then lifted our backpacks up with it to simulate a distributed load and this seemed sufficient, so we used the same techniques with a full scale version.

Figure 13: Small-scale version of netting with paracord edges and carabiner attachments then used to test initial load. The purpose of the small scale version was to prove the concept and plan fabrication before moving forward with a 10x10 ft version.

Having a netting also provided a sufficient attachment point for the drone to be connected to the balloon. We tested this attachment point with Aquiline Drones where a pilot flew the drone over the

netting and pulled on it at different angles, simulating the guiding of the balloon. Our net performed very well in this testing, as seen in Figure 14.

Figure 14: The drone is pulling on the netting material to check for any points of strain or bunching and so that we can verify the netting can withstand being pulled on by the drone.

Full scale testing brings together the lessons learned and final fabricated test articles from previous tests. The first step is fixing the net over the uninflated balloon and anchoring the net to prevent the balloon from floating away. Then we filled the balloon up with helium and ensured the netting did not dislodge. This was also an opportunity to verify the lift calculations performed earlier. Once the balloon was fully inflated, we kept it close to the ground with the netting, and attached the drone tether. Next we tethered the netting to the mannequin harness with the balloon still pulled close to the ground. Once all systems were in working order, we took off with the drone, slowly guided the balloon up to offload the harness, and assessed the system for static stability. Finally, we pulled the mannequin in various directions to assess the active control. Data from the drone's onboard sensors as well as our external sensors were then taken to view numerical depictions of stability and response.

Figure 15: Shots from full scale testing that show filling up the balloon, a group member donning the suit and simulating picking up a box to show what an astronaut would endure during testing.

4.4 Results

Each of our tests informed decisions for either our scale system or a full size system. Each component must take lessons from their respective tests in order to maximize the capabilities of the gravity offload device.

4.4.1 Testing of the drone reveals the innate capabilities of the internal controls. As shown in figures 11 and 12, the drone is capable of maintaining a stable position for both itself and a hanging payload in a strong wind. This shows that we are able to rely on the drone's internal flight control for a lot of stability, and our system only needs to add some feedback from the user.

4.4.2 The netting to be placed over the balloon required various materials tests both qualitative and quantitative. The results of the yield strength test showed polyethylene and the black bird netting to be the two best options. Polyethylene yielded at a load of 7 kg, whereas the black bird netting was able to support over 15 kg. The black netting also provided easy attachment points for our drone tether, as it was simple to grab 4 nodes and attach them to a carabiner. The netting options were also tested for risk of popping the balloon as it rubbed against its surface, and the chosen black netting was soft enough to not be a risk.

4.4.3 The sensors from the BME team were not able to be implemented into the full scale system, but a lot of progress was made. We were able to take sensor acceleration data and integrate it into position data to feed back to a computer. We could also recover roll pitch and yaw data, and show both of these data streams in live time on a computer. The sensors experience some position "drift" with the location data, so they are not suitable for controlling the drone in this format. Hanging the sensor above the subject, as seen in figure 16, would allow us to use the more reliable roll, pitch, and yaw outputs from the sensor. This would turn the controls into an inverted pendulum problem, where any amount of movement would cause the sensor to tilt and this could be calibrated into a movement for the drone.

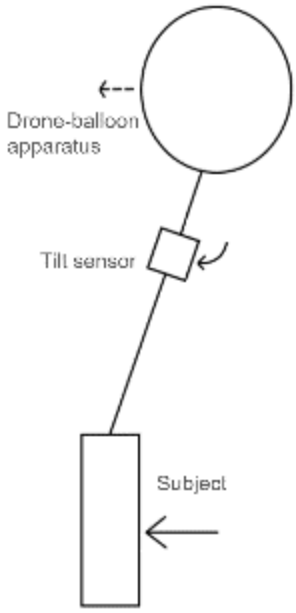

Figure 16: Layout of the sensor in our updated system that uses an inverted pendulum to calibrate the drone's movement to the person.

4.4.4 The final full scale test that we conducted was successful, and was considered a passive full scale test. Weather balloon and the harness were connected together and the drone was not implemented in the system. This tested for offloading force confirmation, harness functionality and comfort, and launch procedures.

4.4.4.1 Initially, we had the harness on the mannequin and were able to move around it with surprising ease and a noticeably reduced weight. This was then verified by a member of our team, who wore the harness and performed relevant movements. Standing, walking, bending over, kneeling, and jumping were all performed with no impedance by the harness or offload. Qualitatively, we noted that there were no major pressure points felt and the offloading of the balloon was naturally applied at their center of gravity. Harness was snug and even in the most difficult relevant movement positions such as bending over and jumping, it still was comfortable. The aluminum arms were present and restricted some arm movement, but it was

determined that an astronaut in training would not need to move their arms in these ways, nor would they be able to while wearing an EVA suit.

4.4.4.2 Offloading force of the system was determined to be 10lbf on the user, which was measured with a spring scale. This was consistent with our calculations for our slightly underinflated balloon with a diameter of about 7ft.

4.4.4.3 Launch procedures are an integral part of determining if the system is able to work as intended. It is noted that our launch conditions were not optimal as there was light rain and some wind, yet the system was still perfectly functional. The materials and subsystems were brought to the launch site. The netting was laid down on the ground, with the protective polyethylene sheeting between the netting and the ground. Carabiners that attached on the sides of the netting were disconnected and left on the sheeting while the corner carabiners were left connected. Weights that totalled to be 150% of the system's offloading force were attached to each corner of the sheeting and netting as safety to hold the balloon down. The helium canisters were brought to the site and set up to connect to the weather balloon. Balloon was placed underneath the netting and above the sheeting and spread out to allow the helium to flow in. This protected the balloon from being in contact with the ground that may otherwise cause tears. Helium flow was started and simultaneously the netting was constantly shifted towards the center of the balloon. As the balloon started to rise off the ground, we connected the harness to each of their respective corners and removed the polyethylene sheeting. The paracord was attached to the harness' swivel bar and tied to the carabiner at each corner. Currently, each corner would be attached to the netting, the safety weights, and the harness. After finishing up inflating the weather balloon, it is important to correctly tie off the nozzle while a person holds it down by the nozzle to prevent the balloon from escaping. This requires folding up the nozzle halfway, and then loop a safety line at the nozzle. Tightly wrap the folded

nozzle with electrical tape and make sure the safety line is still connected. At the other end of the safety line, start to shift over the weights from the netting corners to the safety line. This ensures that the weather balloon is always weighed down during the whole process in case of failure and the balloon escapes. Now is the time to let the weather balloon take off. With individuals holding the balloon down by the harness to netting tethers, slowly let up the balloon into the air. Another person is to move the harness and mannequin underneath the balloon and to allow the swivel bar to rise up. Have the user don the harness and tighten all straps accordingly. These procedures allow for a safe and effective launch of the passive system.

4.4.4.4 If the active system was to be set up, which would include the drone, here are the following changes. The drone would be attached to the center of the netting, and would clip on by the carabiner at the end of the drone tether line. Before the balloon is inflated, connect the drone to the netting. When it is completely inflated and before it is released up into the air, start the drone and fly it above the balloon. The length of the line is 8 feet and should be as large as the diameter of the balloon. Slowly let the balloon rise as people let go of the harness to balloon tether. Keep the drone above the balloon and do not let the line get taut until you start testing. When you want to have the drone land, pull the weather balloon down by the harness to netting tethers while keeping the drone in position. When it is low enough, you can land the drone.

4.4.4.5 A suggestion for the future is to have the drone to netting line be adjustable in length to aid in takeoff procedures as well as longevity of testing periods that were previously limited by the flight time of the drone. This winch would be located at one end of the tether and is able to be remotely controlled to adjust length while handling all desired loading of the system. For example, we will reference the status of equipment at the end of the static system procedures. The tether would be long enough to reach the ground to the drone when the weather balloon is

in flight. Drone would be able to take off and fly above the weather balloon without pulling the tether line taut. When the drone reaches the position above the weather balloon, the tether line would be able to shorten to the desired length. When the testing is over or the drone needs to replace its battery, the winch can lengthen the tether so as to allow the drone to land. This remote-controlled winch allows two problems to be solved. Short drone flight time is solved by easy landing procedures to swap out the battery to quickly continue testing. Safety of drone landing procedures is improved as a longer tether decreases the chance of a drone crash than by a shorter tether.

Figure 17: One Balloon Version: Balloon is 14ft diameter and is able to offload 100 lbf. Tether system would be identical and scaled up from our current system

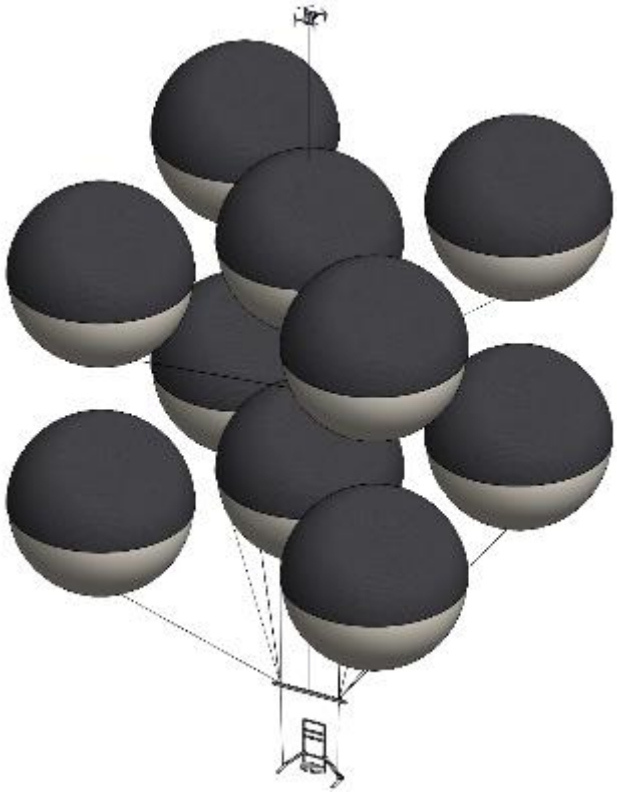

Figure 18: Cluster Ballooning Version: Each balloon is the standard 9ft diameter as we have been using, and is connected through a consolidated tether system. With 10 balloons, this offloads 200lbf

These figures (17-18) showcase renditions of what a full scale system may look like. Larger components of the system can be used to scale upwards, such as a bigger net and a stronger drone which applies to all design versions. A single and larger balloon may be used and inflated to the desired offload of the user. This is the most translatable version and is recommended. The cluster balloon is another method that just connects many balloons to the harness and has been a tested design by cluster balloonists. Overall, the flexibility of the system to adjust the balloons for the offloading total in the system proves to be a strength.

5 Summary

The goal of this project was to create a gravity offload device that is scalable to offload at least 100lbf and could be used to train astronauts in field environments. We set our own goals of being able to offload 25 lbf, have the system be safe and comfortable for the user, allow all relevant movement of an astronaut in training, have the system actively respond to movement and changes in center of mass, and for all of this to work in field environments.

Our system managed to do well in all of these aspects. While we only tested up to 10lbf of offloading, the balloon was capable of lifting more. The flexibility and mobility of the harness and offloading device was completely uninhibiting of all relevant movements. The balloon was passively stable and could respond to movement, and we currently have the framework for implementing a drone with sensors to decrease latency. This is all scalable to NASA's goals and beyond.

Additional tests we would like to conduct if given the opportunity would largely be centered around the sensors. The sensors would likely need a lot of calibration to correlate tilt of the sensor to exact drone response. This should be found through numerous tests pulling the offloaded mannequin and reading the drone's response.

Based on our findings, there are a few design changes that we would implement on a scaled up system in order to maximize performance and safety. First and foremost, more buoyancy force would be required to offload the required 100 lbf. This could be achieved with a larger balloon of about 14ft in diameter or around 4-5 balloons of similar size to our scaled down system. Our recommendation is to use a netting around the balloon that can be completely closed around the bottom, so there is no chance of the balloon slipping out. This would increase the safety and reliability of the system in high wind and movement situations. In order to control the increased size of the scaled up system, more aggressive response coding and/or a more powerful drone would be necessary. Installing a deflector plate above the

harness would further increase the safety of the user by preventing any equipment from falling on them in the event of a failure. Finally, using position sensors that do not experience the “drift” that we noticed in testing in addition to our roll/pitch/yaw sensor would allow for improved accuracy and redundancy for drone controls.

With all of these changes implemented, our design could be successful in creating a reduced gravity analogue for NASA’s field environment training.

6 References

6.1 Works Cited

[1] Tactical Technology Office, C. D. Fritz, R. A. Egen, J. O. Frankosky, and D. K. Blue, Washington, D.C.: National Technical Information Service, 1973.

[2] F. Sibella, I. Frosio, F. Schena, and N. A. Borghese, “3D analysis of the body center of mass in rock climbing,” *Human Movement Science*, vol. 26, no. 6, pp. 841–852, 2007.

6.2 Works Consulted

[3] S. Carhart, D. Cooper, L. Gaitan, M. Kaliterna, S. Lama, P. Rogel-Herrara, and Y. Yabe, “Heavy Lift Drone,” thesis, Interdisciplinary Design Senior Theses., 2020.

[4] P.-J. Bristeau, F. Callou, D. Vissière, and N. Petit, “The navigation and control technology inside the AR.Drone Micro UAV,” *IFAC Proceedings Volumes*, vol. 44, no. 1, pp. 1477–1484, 2011.

[5] Team Edelrid, “Types of climbing harnesses,” *Edelrid*, 23-May-2019. [Online]. Available: https://www.edelrid.de/en/knowledge-base/sports/types-of-climbing-harnesses.php. [Accessed: 22-Oct-2021].

[6] M. Roeggla, M. Brunner, A. Michalek, G. Gamper, I. Marschall, M. M. Hirschl, A. N. Laggner, and G. Roeggla, “Cardiorespiratory response to free suspension simulating the situation between fall and rescue in a rock climbing accident,” *Wilderness & Environmental Medicine*, vol. 7, no. 2, pp. 109–114, 1996.

7 Appendix A- Matlab Code

7.1 Appendix A1- Matlab Code for Drone time of flight

Used in figure 1 within section 4. Calculates the time of flight of a drone based on different masses.

```
mass = linspace(.3,7);

P = 170; %W/kg  (estimate on number of watts required to lift one kg: https://www.omnicalculator.com/other/drone-flight-time)

V = 36; %voltage of batteries

discharge = .80; %percentage of the battery capacity that is discharged

capacity = 5; %amp hours



AverageAmpDraw = mass .* P ./ V; %


time = capacity .* discharge ./ AverageAmpDraw;


plot(mass*2.205, time)

title("Time of Flight vs Weight of Drone+Payload")

xlabel("Weight (lbf)")

ylabel("Time of flight (hr)")
```

7.2 Appendix A2- Matlab Code for Drag force on balloon

Used in figure 3 within section 4. Calculates the drag force on the balloon as it moves laterally with an astronaut in a harness.

```
rho = 1.293; %kg/m3

r = 1.3716; %m

A = pi*r^2; %m2

v = 1.78816; %m/s (this is equal to 4mph which is above the walking speed that we would likely need

cd = .5; %https://www.engineeringtoolbox.com/drag-coefficient-d_627.html
```

```
Fd = .5*cd*rho*A*v^2


m = 1.200 + .1786*4/3*pi*r^3 %mass of balloon plus helium in balloon (kg)


v = 0:.1:2.5;
F = .5* cd*rho*A*v.^2 *0.224809; %converting to lbf
plot(v*2.23694, F) %converted velocity to mph
title("Drag Force Experienced by the Weather Balloon vs Velocity of Astronaut")
xlabel("Velocity (mph)")
ylabel("Force (lbf)")
```

7.3 Appendix A3- Matlab Code for percent error in the unit problem:

Used in tables 1 and 2 and figures 8 and 9 within section 3. Calculates the percent error for the unit problem and graphs some results.

```
E = 2.12 * 10^11;
L = 0.3;
A = 1.96*10^(-5);
F = 450;

dL = F*L/(A*E)


x = [536 765 765 9486];
y = [((dL-.00012827)/dL * -100) ((dL-.00017295)/dL * -100) ((dL-.00017295)/dL * -100) ((dL-
    (3.242*10^-5))/dL * 100)];

plot(x,y)
title("Percent Error vs Number of Elements")
ylabel("Percent Error (%)")
xlabel("Number of Elements")
```

8 Appendix B- Unit Problem

A cantilever beam can be modeled using FEA software like ANSYS for determining the maximum deformation when a force is applied. Finite element analysis (FEA) is a method of finding structural properties by dividing an object into a number of elements, where the calculations are performed at each node. The first task is to model a cantilever beam in ANSYS workbench to determine the maximum deformation.

The second aspect of this unit problem is to use the same FEA software to compute a solution relevant to our project. Because we will be attaching a drone/balloon system to the person, a connection is necessary, which will most likely be some kind of steel wire rope. A wire rope is typically made of non-alloy carbon steel with a carbon content of 0.4 to 0.95%. For the purpose of this experiment, it is assumed that the rope is one solid rod, whereas in reality it will be composed of many fibers woven into each other. This provides a more conservative estimate because cables have a higher tensile strength than rods. The fibers in a steel cable are cold drawn more than something with a larger diameter, which creates smaller and more elongated grains. This causes the fibers to have a hard time moving because they become stuck on the grain boundaries. The rope can be safely assumed as a rod in this simulation because if it can withstand a tensile strength in the shape of a rod, it can most definitely withstand it as a woven cable. The material chosen for the simulation was carbon steel (1060 annealed) because it seems to be the most common material for a steel rope. This will help us to more accurately model a real world problem.

A beam was modeled in ANSYS Workbench with length of 1m, a width of 0.05m, and a height of 0.05m. One side was fixed at the end, where on the other side, a force of 30 kN was applied. This

simulation was solved multiple times with varying mesh sizes for the purpose of comparing with analytical results. Analytically, the solution was solved using the equation for beam deflection, which is below:

$$\delta_{max} = \frac{FL^3}{3EI} \quad [4]$$

Where δ_{max} is the maximum deflection (m), L is the length of the beam (m), E is the Young's modulus ($2 \times 10^{11}\ N/m^2$), and I is the moment of inertia (m^4) which is solved using Equation 5.

$$I = \frac{w * h^3}{12} \quad [5]$$

Where w is the width of the beam (m) and h is the height of the beam (m). The maximum deflection was calculated using a MATLAB code (see appendix). The analytical solution will then be compared with the numerical results, which will relate the size of the mesh to the accuracy of the numerical solution. It is expected that as mesh size increases, the accuracy increases because the finite element method is meant to assume infinite elements.

The simulations were run at different element sizes and compared to the analytical solution. The analytical solution was used as the control variable. Evidently, the greater the number of elements, the smaller the percent error. Each simulation performed is shown below.

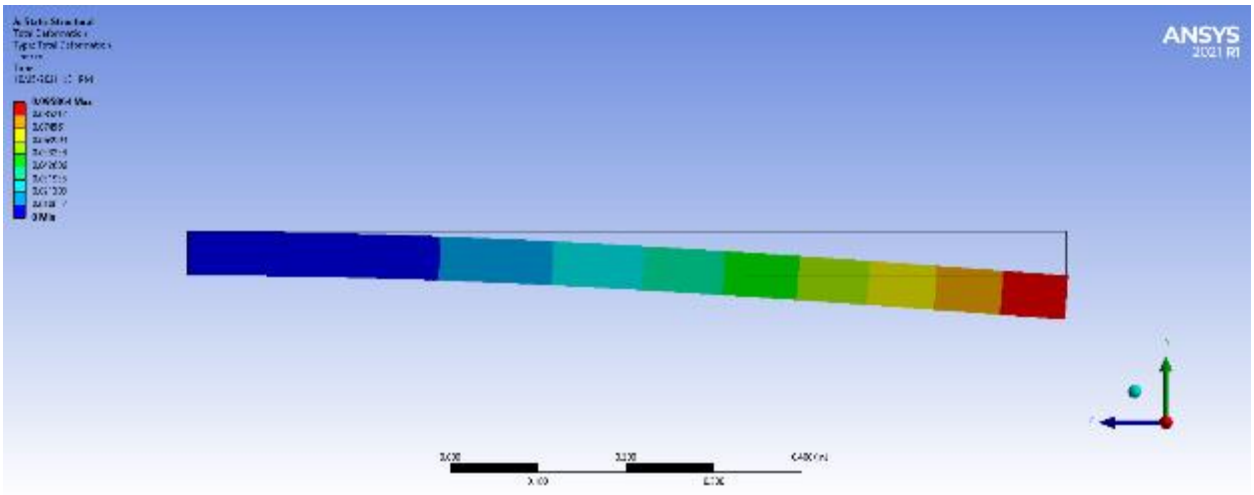

Figure 10: Total deformation of cantilever beam with a mesh size of 0.02m

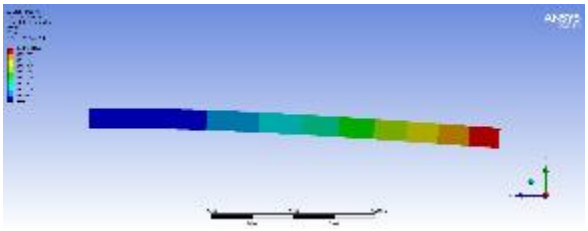

Figure 11: Total deformation of cantilever beam with a mesh size of 0.05m

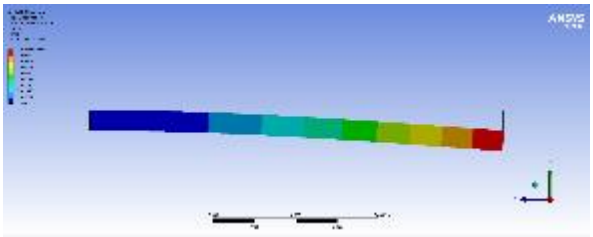

Figure 12: Total deformation of cantilever beam with a mesh size of 0.01m

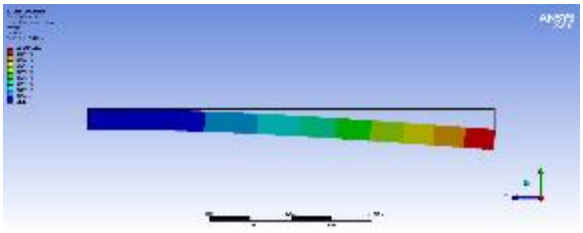

Figure 13: Total deformation of cantilever beam with a mesh size of 0.005m

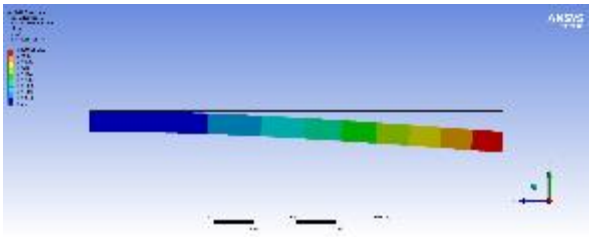

Figure 14: Total deformation of cantilever beam with a mesh size of 0.0025m

Table 2: FEA Beam Analysis

Element Size (m)	Number of Elements	Analytical Solution (m)	FEA Solution (m)	Percent Error (%)
.049968	84	.096000	.095734	.277
.02	450	.096000	.095864	.142
.01	2500	.096000	.095911	.0927
.005	20000	.096000	.095938	.0646
.0025	160000	.096000	.095951	.0510

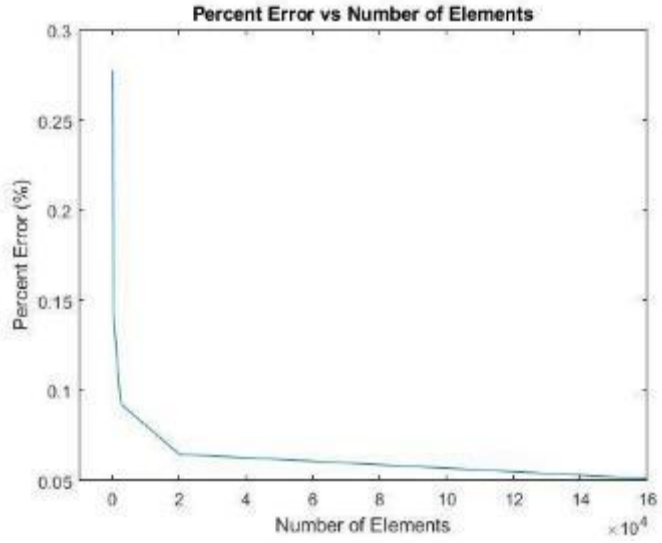

Figure 15: The graph above shows the number of elements vs the percent error of the numerical solution.

As expected, as the number of nodes increases, the percent error decreases, meaning the numerical solution is more accurate. The most significant decrease in error occurs from zero to 2×10^4 elements. This range experiences a sharp, exponential dropoff. This still leaves us with less than 0.1% error which is quite accurate. For the purposes of this project, this threshold is sufficient.

A steel rod was modeled in ANSYS with one fixed end and a tensile load pulling in the axial direction on the other end. The beam has a diameter of .005m, a length of .3m and it is made out of carbon steel 1060. The material choice was based on the material used to make steel cables. A solid cylinder would be less strong than an actual wound cable, so this was used as a conservative estimate.

The following equation was used to calculate the elongation of the cable.

$$\Delta L = \frac{FL}{AE} \quad [6]$$

where F is the tensile load (450N), L is the length of the beam (0.3m), A is the cross sectional area ($1.96 \cdot 10^{-5}$), and E is the Young's Modulus ($2.12 \cdot 10^{11}$ Pa). This equation was solved analytically and the solutions were compared to the ANSYS results.

Additionally, the ANSYS model was used to calculate the stress in the cable to further evaluate the performance. The results of the simulation showed minimal deformation under realistic tensile stress. The following figure/table was derived.

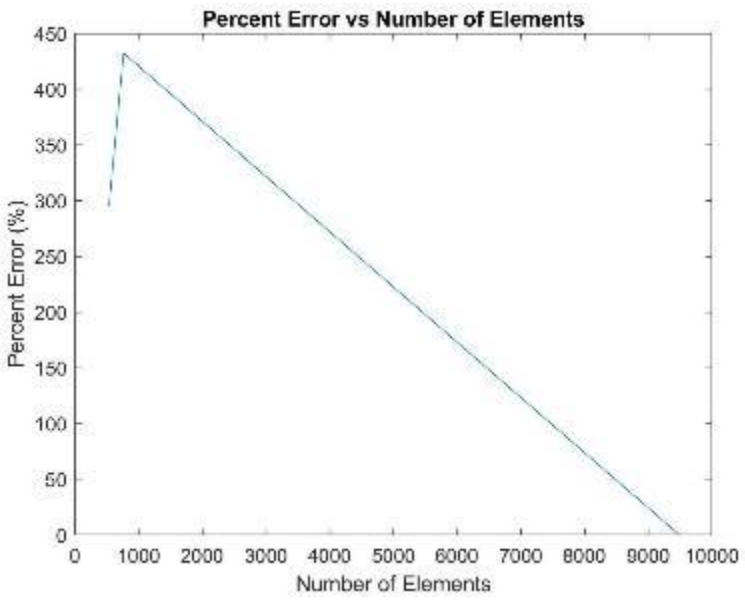

Figure 16: Plot of Percent Error vs Number of Elements.

Table 3

Element Size (m)	Number of Elements	Analytical Solution (m)	FEA Solution (m)	Percent Error (%)
.0025	536	$3.25 \cdot 10^{-5}$	$1.28 \cdot 10^{-5}$	290
.01	765	$3.25 \cdot 10^{-5}$	$1.73 \cdot 10^{-5}$	430
.005	765	$3.25 \cdot 10^{-5}$	$1.73 \cdot 10^{-5}$	430
.001	9486	$3.25 \cdot 10^{-5}$	$3.24 \cdot 10^{-5}$	.21

The unusual trend at the beginning of the graph in figure 16 is likely due to an error in the calculated number of elements from ANSYS. As is seen in table 3, the reported number of elements is fewer when their size is .0025m compared to when the size is a larger .01m. This is not consistent with how the geometry should play out, meaning there was likely either a glitch within ANSYS showing the wrong number of elements, or a human error in translation. Ignoring this data point otherwise shows the expected downward trend of error with decreasing element size.

As seen in figure 10, the rod bends slightly under an applied tensile load. Given the desired nature of this force, there should be no bending, so this must be a result of the ANSYS parameters. If the mesh size is too small, the tensile force is not able to be anchored to a central point on the rod, causing an asymmetrical load. This leads to bending and more deformation. The geometry of the meshes also contributes to the inconsistent trend in the percent error of the deformation. There should be no reason for this type of bending in a physical system.

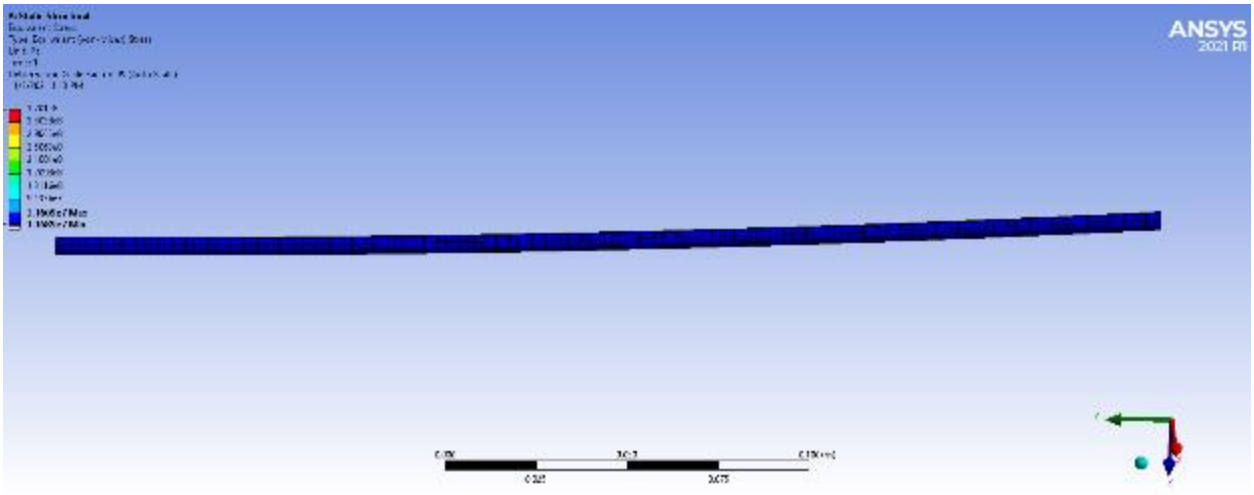

Figure 17: The steel rod undergoing a realistic tensile stress. The contour has been changed to represent the yield strength of the material, so the points of failure would be represented by the color red. However, it is clear in this photo that there is virtually no risk of failure in this simulation.

Based on the data from this model, it is possible to conclude that a cantilever beam would experience some deformation when a force is applied directly to one end using FEA software. We also note that increasing the number of elements will reduce the percent error. Although increasing the number of elements increases the time spent to solve the simulation, this is offset by the fact that our geometry is not very complex in this situation, so adding elements does not add too much time. The same method can be applied to future designs of our project, as it is important to be sure that our designs will not experience deformation when a load is applied, which was demonstrated by the tensile strength simulation. This will be important in determining the material being used for our rig, as we know how much force will be applied. The material chosen will need to be able to withstand a certain force without experiencing deformation. Because the force we will be applying is not very large, deformation is not expected, although it is something to consider before actually building our project. Minimizing deformation is essential, and performing FEA beforehand will save us time and material costs during the prototyping phase.